JOURNAL OF SYNCHROTRON RADIATION
ISSN 1600-5775

Finite lifetime broadening of calculated X-ray absorption spectra: possible artefacts close to the edge

Ondřej Šipr,[a]* Jiří Vackář[b] and Ján Minár[c]

[a]Institute of Physics, Czech Academy of Sciences, Cukrovarnická 10, CZ-162 53 Prague, Czech Republic, [b]Institute of Physics, Czech Academy of Sciences, Na Slovance 2, CZ-182 21 Prague, Czech Republic, and [c]University of West Bohemia, Univerzitní 8, CZ-306 14 Pilsen, Czech Republic.
*Correspondence e-mail: sipr@fzu.cz

Received 22 September 2017
Accepted 2 January 2018

Edited by R. W. Strange, University of Essex, UK

Keywords: X-ray absorption spectroscopy; core hole lifetime; multiple-scattering formalism.

X-ray absorption spectra calculated within an effective one-electron approach have to be broadened to account for the finite lifetime of the core hole. For methods based on Green's function this can be achieved either by adding a small imaginary part to the energy or by convoluting the spectra on the real axis with a Lorentzian. By analyzing the Fe K- and $L_{2,3}$-edge spectra it is demonstrated that these procedures lead to identical results only for energies higher than a few core-level widths above the absorption edge. For energies close to the edge, spurious spectral features may appear if too much weight is put on broadening *via* the imaginary energy component. Special care should be taken for dichroic spectra at edges which comprise several exchange-split core levels, such as the L_3-edge of 3d transition metals.

1. Introduction

Generally, experimental X-ray absorption spectra (XAS) contain fewer structures and display broader features than theoretical spectra. This is because the finite lifetime of the core hole is usually neglected in the calculations. To facilitate proper comparison between theory and experiment, the calculated spectrum is modified so that the finite core hole lifetime is accounted for. A convenient way to achieve this is to convolute the raw spectrum *a posteriori* with a Lorentzian (Messiah, 1962). This is a well established procedure. Its drawback is that sometimes one has to perform the calculation on a much finer energy mesh than is actually needed: the raw spectrum contains many fine and sharp features that will be smeared out eventually but which, nevertheless, have to be included in the calculated spectrum before the final broadening is applied.

For Green's-function-based or multiple-scattering methods, there is another, computationally more efficient, way to account for the finite core hole lifetime, namely by adding a small imaginary part to the energy (Messiah, 1962; Brouder *et al.*, 1996; Natoli *et al.*, 2003; Sébilleau *et al.*, 2006). This will result in smoother spectra from the beginning, meaning that one can use a coarser energy mesh. Another technical advantage of this approach is that, when working in reciprocal space, employing complex energies may significantly reduce the number of **k**-points needed for an accurate Brillouin zone integration. The option to use complex energies is available in several codes designed for XAS calculations, among others, in *FDMNES* (Joly, 2015; Bunău & Joly, 2009), *FEFF* (Rehr, 2013; Rehr *et al.*, 2009), *MsSpec* (Sébilleau, 2017; Sébilleau *et al.*,

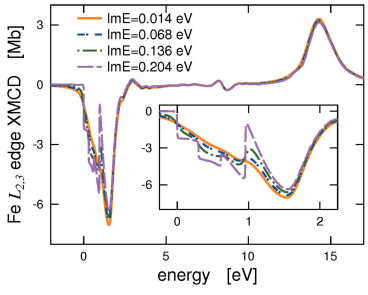

2011), *MXAN* (Benfatto & Della Longa, 2003; Benfatto *et al.*, 2003) or *SPRKKR* (Ebert, 2017; Ebert *et al.*, 2011). Often one can combine both approaches by first calculating the spectrum using an imaginary energy component to achieve basic reduction of the computer workload and then by convoluting it with a Lorentzian to achieve the best possible agreement with experiment.

The problem with calculating X-ray absorption spectra for energies with an added imaginary component is that this procedure is formally equivalent to a convolution with a Lorentzian only if there is no cut-off of the spectra below the Fermi level E_F, *i.e.* in the limit $E_F \rightarrow -\infty$ (Brouder *et al.*, 1996). Usually this circumstance is tacitly ignored because the influence of the cut-off is negligible sufficiently above the edge. Specifically, this applies to the whole extended X-ray absorption fine-structure (EXAFS) region. However, the question remains whether and under what circumstances the employment of an imaginary energy component might lead to undesirable artefacts at the very edge. Brouder *et al.* (1996) derived an equation linking XAS calculated for complex energies to XAS obtained by convolution of spectra on the real axis which takes into account the influence of the cut-off below E_F. Their equation contains a correction factor which could in principle be calculated but which is normally ignored. An analysis of how serious this neglect might be has not been presented so far.

The finite core hole lifetime is not the only factor that contributes to the broadening of spectra. Other effects to consider are, for example, finite lifetime of the excited photoelectron or thermal vibrations. The broadening caused by the finite core hole lifetime is, nevertheless, the dominant broadening process close to the edge, and knowing the limitations of procedures used to account for it is desirable.

Our aim is to assess whether employment of an imaginary energy component to calculate broadened X-ray absorption spectra can introduce significant artefacts in comparison with broadening by a convolution of raw spectra calculated on the real axis. To cover a range of circumstances, we investigate Fe *K*-edge and Fe $L_{2,3}$-edge XAS and X-ray magnetic circular dichroism (XMCD). We will show that if the dominant mechanism of the broadening is adding an imaginary part to the energy, spurious spectral features may appear close to the edge. This is especially the case for dichroic spectra at edges which comprise several exchange-split core levels of small natural widths, as it is for the case of the L_3-edges of 3*d* transition metals, for example.

2. Methods

Fe *K*-edge and Fe $L_{2,3}$-edge XAS and XMCD spectra were calculated using an *ab initio* fully relativistic multiple-scattering Green's function method, as implemented in the *SPRKKR* code (Ebert, 2017; Ebert *et al.*, 2011). We are dealing with crystals, so the calculations were performed in reciprocal space. The **k**-space integrals were carried out using 36000 points in the full Brillouin zone. Multipole expansion of the Green's function was cut at $\ell_{max} = 2$. We checked that these values are sufficient. The influence of the core hole on the potential was ignored, which is justified for our purpose; quantitative estimate of the core hole effect has been given, for example, by Zeller (1988) for the Fe *K*-edge and by Šipr *et al.* (2011) for the Fe $L_{2,3}$-edge.

Use of a fully relativistic formalism means that the core levels associated with absorption edges are non-degenerate, separated by exchange splitting. For the *K*-edge, core levels characterized by relativistic quantum numbers $\kappa = -1$, $\mu = \pm 1/2$ are split by 0.005 eV. For the L_2-edge, core levels characterized by $\kappa = 1$, $\mu = \pm 1/2$ are split by 0.3 eV. For the L_3-edge, the four levels characterized by $\kappa = -2$, $\mu = \pm 1/2, \pm 3/2$ are also split by about 0.3 eV from each other, spanning the total range of 1 eV. We will see that this exchange splitting of core levels contributes to the possible emergence of artefacts close to the edge if the spectra are broadened by employing complex energies.

As noted in the *Introduction*, there are two ways to simulate the effect of the finite core hole lifetime on X-ray absorption spectra. First, it is the convolution of the raw spectrum calculated for real photoelectron energies by a Lorentzian $L(E)$. If the full width at half-maximum (FWHM) of the Lorentzian is Γ, it can be written as

$$L(E) = \frac{1}{\pi} \frac{\Gamma/2}{E^2 + (\Gamma/2)^2}. \tag{1}$$

Starting with a raw X-ray absorption cross section $\sigma_{raw}(E)$ which ignores the finite core lifetime effects, one makes a convolution

$$\sigma_{broad}(E) = \int_{E_F}^{\infty} \mathrm{d}E' \, \sigma_{raw}(E') \, L(E - E') \tag{2}$$

to obtain the cross section $\sigma_{broad}(E)$ where the influence of the finite core hole lifetime has been included.

It can be shown that if the cut-off at E_F is ignored in equation (2), the effect of the finite core hole lifetime can be equivalently accounted for by evaluating the X-ray absorption cross section for energies with added imaginary component $\Gamma/2$ (Messiah, 1962; Brouder *et al.*, 1996; Natoli *et al.*, 2003; Sébilleau *et al.*, 2006). In other words,

$$\int_{-\infty}^{\infty} \mathrm{d}E' \, \sigma_{raw}(E') \, L(E - E') = \sigma_{raw}(E + i\Gamma/2). \tag{3}$$

The X-ray absorption cross section with the influence of finite core lifetime included is thus taken as

$$\sigma_{broad}(E) \simeq \sigma_{raw}(E + i\Gamma/2). \tag{4}$$

We want to test to what degree one can use equation (4) instead of equation (2), saving thus computer resources and increasing the numerical stability of the results. For this purpose we distribute the required core level broadening between the procedures described by equations (2) and (4), with various weights. This can be done consistently because a convolution of two Lorentzians with FWHMs of Γ_1 and Γ_2 is again a Lorentzian, with FWHM equal to $\Gamma_1 + \Gamma_2$. So if we want to simulate a total core hole broadening Γ_{core}, we employ first equation (4) with an imaginary energy part $\mathrm{Im}\, E$ and then

Table 1
Parameters (in eV) used for broadening the Fe *K*-edge spectra by including the imaginary part $\mathrm{Im}\,E$ to the energy and by subsequent convolution of the calculated spectra with a Lorentzian of width Γ_K.

Values are chosen so that the total (combined) broadening determined by equation (5) corresponds to $\Gamma_{\rm core} = 1.19$ eV.

$\mathrm{Im}\,E$	Γ_K	$2\,\mathrm{Im}\,E + \Gamma_K$
0.014	1.163	1.190
0.272	0.646	1.190
0.408	0.374	1.190
0.594	0.002	1.190

Table 2
As Table 1 but for the $L_{2,3}$-edge.

Values are chosen so that the total broadening determined by equation (5) corresponds to $\Gamma_{\rm core} = 1.14$ eV for the L_2-edge and to $\Gamma_{\rm core} = 0.41$ eV for the L_3-edge.

$\mathrm{Im}\,E$	Γ_{L_2}	Γ_{L_3}	$2\,\mathrm{Im}\,E + \Gamma_{L_2}$	$2\,\mathrm{Im}\,E + \Gamma_{L_3}$
0.014	1.113	0.383	1.140	0.410
0.068	1.004	0.274	1.140	0.410
0.136	0.868	0.138	1.140	0.410
0.204	0.732	0.002	1.140	0.410

convolute the spectrum with a Lorentzian of width Γ, requiring that

$$2\,\mathrm{Im}\,E + \Gamma = \Gamma_{\rm core}. \qquad (5)$$

In our case we take $\Gamma_{\rm core} = 1.19$ eV for the Fe *K*-edge, $\Gamma_{\rm core} = 1.14$ eV for the Fe L_2-edge and $\Gamma_{\rm core} = 0.41$ eV for the Fe L_3-edge (Campbell & Papp, 2001). The values of $\mathrm{Im}\,E$ and Γ used for studying the Fe *K*-edge are shown in Table 1, and the values used for studying the Fe $L_{2,3}$-edge are shown in Table 2. The rationale for selecting these particular values is that in this way we include both extreme situations when the broadening is incorporated either solely *via* the Lorentzian convolution or solely *via* the imaginary energy component, together with two intermediate situations. Note that for the $L_{2,3}$-edge spectra the convolution is performed separately for the L_2-edge and L_3-edge and only then are both spectra merged.

3. Results: Fe *K*-edge and $L_{2,3}$-edge XAS and XMCD

3.1. Total spectra (unresolved in κ or μ)

We start by inspecting how shifting the weight of the broadening from a Lorentzian convolution to an imaginary energy component affects the calculated XAS and XMCD. This is done in Fig. 1 for the Fe *K*-edge and in Fig. 2 for the Fe $L_{2,3}$-edge. We focus solely on the theoretical spectra; a good agreement of theory with experiment was demonstrated earlier (Šipr & Ebert, 2005; Šipr *et al.*, 2011).

One can see that for energies higher than about $5\Gamma_{\rm core}$ above the edge there is practically no difference in the spectra, no matter which broadening procedure has been applied. At the very edge, however, there are differences. They stem from the fact that, if too much weight is put on broadening by means of the imaginary energy component, there is a sharp cut-off of

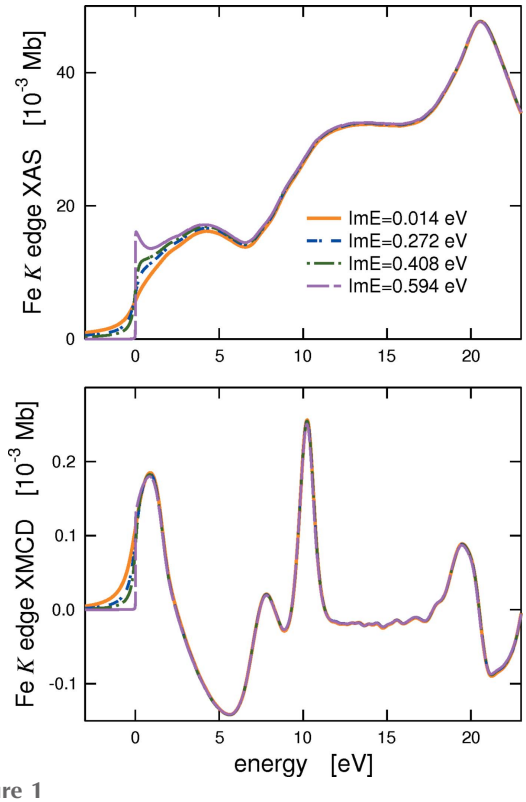

Figure 1
Fe *K*-edge XAS and XMCD calculated for different imaginary energies and convoluted subsequently with Lorentzians chosen so that the total spectral broadening $2\,\mathrm{Im}\,E + \Gamma_K$ remains constant.

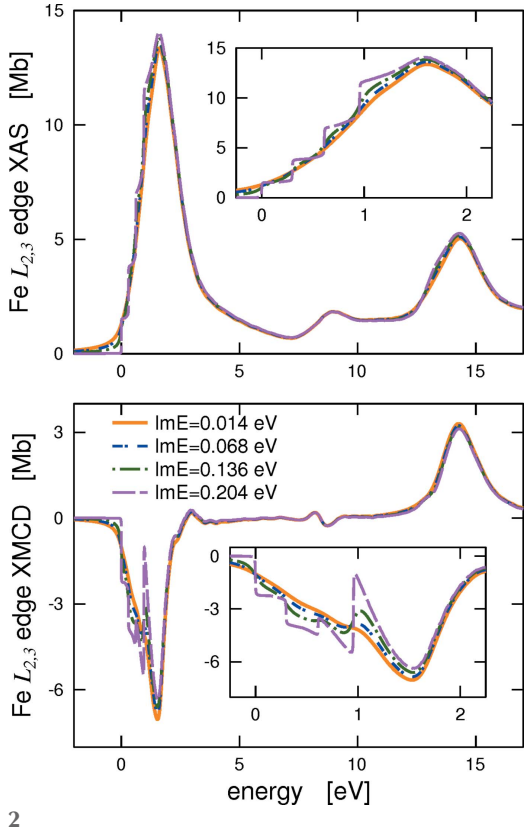

Figure 2
As Fig. 1 but for the $L_{2,3}$-edge. The insets show detailed views of the L_3-edge region.

the spectra at E_F, resulting in too sharp features at the edge. If a sufficient amount of broadening is performed *via* Lorentzian convolution, this cut-off is smeared out.

The situation is especially instructive for the Fe L_3-edge XMCD peak. Here a well distinguished but in fact spurious fine structure appears on its low-energy side unless most of the broadening is performed by means of Lorentzian convolution. The situation is much less dramatic for the corresponding XAS peak. This is because of the way the XMCD peak is generated: it is a sum of four (L_3-edge) or two (L_2-edge) contributions which may have opposite signs and which have their edges at slightly different energies due to the relativistic exchange splitting of the core levels.

3.2. (κ,μ)-resolved spectra

An insight can be obtained by looking at individual (κ,μ)-components contributing to the Fe $L_{2,3}$-edge XAS and XMCD for the two extreme cases, with Im E = 0.204 eV (nearly all broadening done *via* the imaginary energy component) and with Im E = 0.014 eV (nearly all broadening done *via* a convolution with a Lorentzian, *cf.* Table 2). If one looks at the spectra obtained using Im E = 0.204 eV (Fig. 3), one can see that the individual components indeed exhibit sharp edges or onsets at different energies. If all components have the same sign, as is the case of XAS, the resulting spectrum is 'rugged'

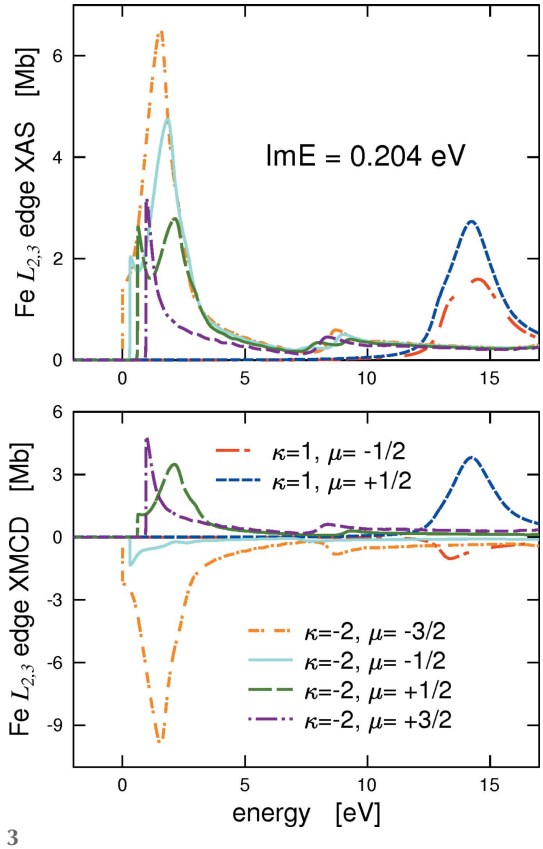

Figure 3
(κ,μ)-decomposed Fe $L_{2,3}$-edge XAS and XMCD calculated for imaginary energy 0.204 eV and convoluted subsequently with Lorentzians of Γ_{L_2} = 0.732 eV (for the L_2-edge) and Γ_{L_3} = 0.002 eV (for the L_3-edge).

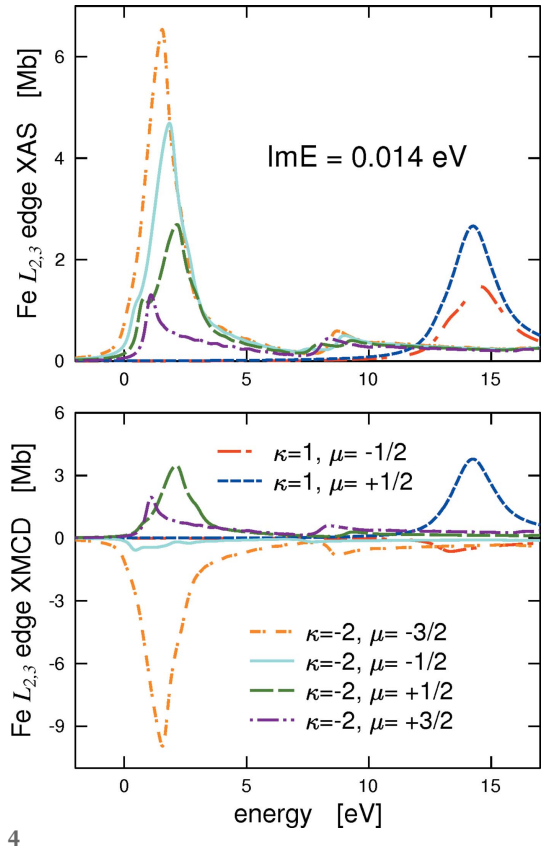

Figure 4
As Fig. 3 but for for imaginary energy 0.014 eV and Lorentzian widths Γ_{L_2} = 1.113 eV and Γ_{L_3} = 0.383 eV for the L_2- and L_3-edges, respectively.

but in general not so much different from the spectra obtained for smaller Im E (see the upper panel in Fig. 2). However, if the individual (κ,μ) components differ in sign as in the case of XMCD, their sum may give rise to a spectrum which is significantly different from the spectrum obtained for smaller Im E (the lower panel in Fig. 2). Technically, this difference can be understood by comparing Fig. 3 with Fig. 4, which is its analog but with a smaller imaginary energy part Im E = 0.014 eV. One can see that if the individual (κ,μ)-components have been smoothed *before* the summation, the resulting spectrum is smooth as well, without the quasi-oscillation at about 1 eV which appears in the XMCD spectrum for larger Im E values (*cf.* Fig. 2).

4. Discussion

Our aim was to check whether the employment of complex energies for calculating broadened XAS and XMCD spectra can introduce significant distortions in comparison with what is obtained by convoluting the spectra calculated on the real axis. Our results indicate that simulating the finite core hole lifetime by means of an imaginary energy component and by means of convoluting the raw spectra with a Lorentzian is equivalent only for energies higher than a few core level FWHMs above the absorption edge. If too much weight is put on broadening *via* an imaginary energy component, spurious

spectral features may appear close to the edge, especially for the dichroic spectra.

When contemplating practical implications, one should realize that there are other sources of spectral broadening that we did not consider. An important factor is the photelectron mean free path related to its finite lifetime. Various methods have been used to describe the photoelectron inelastic mean free path, either by *ab initio* methods such as the GW (Sorini *et al.*, 2006; Zhukov *et al.*, 2006) or employing more intuitive models (Chantler & Bourke, 2014). Calculating XAS using *ab initio* methods that include strong correlations also results in spectra that are broader than what is obtained using the effective one-electron approach (Pardini *et al.*, 2011; Šipr *et al.*, 2011). The usual way to account for the finite photoelectron lifetime is to proceed similarly as in the case of the core hole lifetime, namely to apply an additional (possibly energy-dependent) broadening (Müller *et al.*, 1982). Another contribution to the broadening which, unlike the case of the finite photoelectron lifetime, cannot be simply added to the core hole lifetime broadening comes from thermal atomic vibrations (Beni & Platzman, 1976; Fujikawa *et al.*, 1999; Šipr *et al.*, 2016). Also in this respect important progress towards an *ab initio* description had been made (Filipponi *et al.*, 1995; Dimakis & Bunker, 1998; Vila *et al.*, 2007). The influence of both effects will be, nevertheless, small at the very edge, which is the region where there is the largest likelihood that the ansatz equation (4) will be inappropriate. In any case our analysis concerns the equivalency of the two ways to broaden the spectra in general [*cf.* equations (2) and (4)], without any necessity to specify the source of the broadening.

Another factor important for comparison with experiment is the instrumental broadening. The effect of the detector is usually accounted for by a Gaussian smearing. Typical values for the width of the Gaussian are 0.8 eV for the Fe *K*-edge and 0.2 eV for the Fe $L_{2,3}$-edge. Applying the instrumental broadening would thus remove most of the significant differences between individual spectra shown in Fig. 1 and also between the XAS spectra shown in the upper panel of Fig. 2. However, the spurious fine structure appearing for large Im E values at the low-energy side of the Fe L_3-edge XMCD peak would remain.

Typical values of the imaginary energy component used for XAS/XMCD calculations are Im $E \simeq$ 0.1–0.2 eV. It follows from our results that, while this is appropriate for most situations, problems might occur for edges where the core hole lifetime broadening is small, such as the L_3-edges of 3*d* transition metals. Special care should be taken for XMCD spectra: it is still reasonable to perform the calculations for complex energies to reduce the computing workload but Im E should be about 0.01 eV or less.

The severity of the effect investigated here increases if the applied core hole lifetime broadening $\Gamma_{\rm core}$ decreases. For example, if we had used FWHMs recommended by an older compilation of Shamma *et al.* (1992) which are about 50% less than the values recommended by the newer compilation of Campbell & Papp (2001), the spurious fine structure at the Fe L_3-edge XMCD peak would be even more pronounced. On the other hand, the fact that core hole lifetime widths are usually not known very accurately means that the effect explored here may be overlooked: if redundant structures appear close to the edge, one might be tempted to apply additional broadening mechanically, without considering that one may be actually dealing with an artefact caused by the mechanism analyzed here.

Finally, the fact that both ways of dealing with core hole lifetime broadening are equivalent sufficiently high above the edge justifies formally the use of exponential damping in the EXAFS region (Lee *et al.*, 1981). Namely, it can be shown that if the free-electron Green's function is evaluated for a complex energy $E + i\Gamma/2$, it gives rise to exponential damping of the photoelectron probability with the mean free path λ (Müller *et al.*, 1982; Natoli *et al.*, 2003; Sébilleau *et al.*, 2006),

$$\lambda = \frac{\hbar}{\Gamma}\left(\frac{2E}{m}\right)^{1/2}. \qquad (6)$$

This leads straightforwardly to the $\exp(-R/\lambda)$ factor used in the EXAFS formula (Lee *et al.*, 1981; Natoli *et al.*, 2003). One only has to take care of whether the mean free path λ is related to the photoelectron probability as it is the case here or whether it is related to the amplitude [then the proper factor is $\exp(-2R/\lambda)$].

5. Conclusions

Well above the absorption edge, the two ways of incorporating the finite core hole lifetime into calculation of X-ray absorption spectra, namely *via* adding an imaginary component to the energy and *via* convoluting the raw spectrum with a Lorentzian, are equivalent. However, this is not the case close to the edge. Ignoring this can lead to the emergence of spurious spectral features. Special care should be taken for dichroic spectra at edges which comprise several exchange-split core levels, as is the case of the L_3-edge of 3*d* transition metals.

Funding information

Funding for this research was provided by: Ministerstvo školství, mládeže a tělovýchovy (MŠMT) LD-COST CZ (grant No. LD15097); Grantová Agentura České Republiky (GAČR) (grant No. 17-14840S); Computational and Experimental Design of Advanced Materials with New Functionalities (CEDAMNF) (grant No. CZ.02.1.01/0.0/0.0/15_003/0000358).

References

Benfatto, M. & Della Longa, S. (2003). *The MXAN code*, http://www.esrf.eu/computing/scientific/MXAN.
Benfatto, M., Della Longa, S. & Natoli, C. R. (2003). *J. Synchrotron Rad.* **10**, 51–57.
Beni, G. & Platzman, P. M. (1976). *Phys. Rev. B*, **14**, 1514–1518.
Brouder, C., Alouani, M. & Bennemann, K. H. (1996). *Phys. Rev. B*, **54**, 7334–7349.
Bunău, O. & Joly, Y. (2009). *J. Phys. Condens. Matter*, **21**, 345501.

Campbell, J. L. & Papp, T. (2001). *At. Data Nucl. Data Tables*, **77**, 1–56.
Chantler, C. T. & Bourke, J. D. (2014). *Phys. Rev. B*, **90**, 174306.
Dimakis, N. & Bunker, G. (1998). *Phys. Rev. B*, **58**, 2467–2475.
Ebert, H. (2017). *The SPRKKR code*, version 7.7. http://ebert.cup.uni-muenchen.de/SPRKKR.
Ebert, H., Ködderitzsch, D. & Minár, J. (2011). *Rep. Prog. Phys.* **74**, 096501.
Filipponi, A., Di Cicco, A. & Natoli, C. R. (1995). *Phys. Rev. B*, **52**, 15122–15134.
Fujikawa, T., Rehr, J., Wada, Y. & Nagamatsu, S. (1999). *J. Phys. Soc. Jpn*, **68**, 1259–1268.
Joly, Y. (2015). *The FNMNES code*, http://neel.cnrs.fr/spip.php?rubrique1007&lang=en.
Lee, P. A., Citrin, P. H., Eisenberger, P. & Kincaid, B. M. (1981). *Rev. Mod. Phys.* **53**, 769–806.
Messiah, A. (1962). *Quantum Mechanics*, Vol. 2, p. 992. Amsterdam: North-Holland.
Müller, J. E., Jepsen, O. & Wilkins, J. W. (1982). *Solid State Commun.* **42**, 365–368.
Natoli, C. R., Benfatto, M., Della Longa, S. & Hatada, K. (2003). *J. Synchrotron Rad.* **10**, 26–42.
Pardini, L., Bellini, V. & Manghi, F. (2011). *J. Phys. Condens. Matter*, **23**, 215601.
Rehr, J. J. (2013). *The FEFF code*, version 9. http://feffproject.org.
Rehr, J. J., Kas, J. J., Prange, M. P., Sorini, A. P., Takimoto, Y. & Vila, F. (2009). *C. R. Phys.* **10**, 548–559.
Sébilleau, D. (2017). *The MsSpec code*, https://ipr.univ-rennes1.fr/msspec?lang=en.
Sébilleau, D., Gunnella, R., Wu, Z.-Y., Matteo, S. D. & Natoli, C. R. (2006). *J. Phys. Condens. Matter*, **18**, R175–R230.
Sébilleau, D., Natoli, C., Gavaza, G. M., Zhao, H., Da Pieve, F. & Hatada, K. (2011). *Comput. Phys. Commun.* **182**, 2567–2579.
Shamma, F. A., Abbate, M. & Fuggle, J. C. (1992). *Unoccupied Electron States*, edited by J. C. Fuggle & J. E. Inglesfield, p. 347. Berlin: Springer Verlag.
Šipr, O. & Ebert, H. (2005). *Phys. Rev. B*, **72**, 134406.
Šipr, O., Minár, J., Scherz, A., Wende, H. & Ebert, H. (2011). *Phys. Rev. B*, **84**, 115102.
Šipr, O., Vackář, J. & Kuzmin, A. (2016). *J. Synchrotron Rad.* **23**, 1433–1439.
Sorini, A. P., Kas, J. J., Rehr, J. J., Prange, M. P. & Levine, Z. H. (2006). *Phys. Rev. B*, **74**, 165111.
Vila, F. D., Rehr, J. J., Rossner, H. H. & Krappe, H. J. (2007). *Phys. Rev. B*, **76**, 014301.
Zeller, R. (1988). *Z. Phys. B*, **72**, 79–85.
Zhukov, V. P., Chulkov, E. V. & Echenique, P. M. (2006). *Phys. Rev. B*, **73**, 125105.